Photoproduction of π^0 on Hydrogen with CLAS $e^+e^-(\gamma)$ detection mode

Michael C. Kunkel,[1,*] Moskov J. Amaryan,[1,†] Igor I. Strakovsky,[2] James Ritman,[3,4] and Gary R. Goldstein[5]

[1] *Old Dominion University, Norfolk, VA 23529, USA*
[2] *The George Washington University, Washington, DC 20052, USA*
[3] *Institut für Kernphysik, Forschungszentrum Jülich, 52424 Jülich, Germany*
[4] *Institut für Experimentalphysik I, RuhrUniversität Bochum, 44780 Bochum, Germany*
[5] *Tufts University, Medford, MA 02155, USA*

Abstract

We report the first high precision measurement of the exclusive π^0 photoproduction cross section via Dalitz decay and e^+e^- pair conversion mode on a hydrogen target in a wide kinematic range with the CLAS setup at Thomas Jefferson National Accelerator Facility. The measurement was performed in the reaction $\gamma p \to pe^+e^-X(\gamma)$ using a tagged photon beam spanning an energy interval from the "resonance" to the "Regge" regimes, i.e photon energies $E = 1.25 - 5.55$ GeV. The final state particles particles $p; e^+; e^-$ were detected while the photon was not detected. The π^0 is identified by analyzing the missing mass of proton. This new data sample quadrupled the world bremsstrahlung database above E = 2 GeV. Our data appear to favor the Regge pole model and the constituent counting rule while disfavoring the Handbag model.

PACS numbers: 12.38.Aw, 13.60.Rj, 14.20.-c, 25.20.Lj

The rich $\pi + N$ resonance spectrum for center-of-mass (c.m.) energies up to 2.5 GeV provides insights and challenges concerning the workings of the strong interaction through partial wave expansions, exchange potentials, non-relativistic quark models and QCD. The π^0 and η photoproduction have always been a complementary tool to investigate and constrain the various models and to lead to further insights. At the interface between the crowded low energy resonance cross section and the smooth higher energy, small angle behavior, traditionally described by Regge poles [1], lies a region in which hadronic duality interpolates the varying cross section behavior. Exclusive π photoproduction and π nucleon elastic scattering show this duality in a semi-local sense through Finite Energy Sum Rules (FESR) [2]. The connection to QCD is more tenuous for on-shell photoproduction of pions at small scattering angles, but the quark content can become manifest through large fixed angle dimensional counting rules [3] as well as being evident in semi-inclusive or exclusive electroproduction of pions, described through Transverse Momentum Distributions (TMDs) and Generalized Parton Distributions (GPDs).

The Regge pole description of photoproduction amplitudes has a long and varied history. For π^0 and η photoproduction, all applications rely on a set of known meson Regge poles. There are two allowed t-channel J^{PC} quantum numbers series, the odd-signature 1^{--} and the 1^{+-}, corresponding to the ρ^0, ω, and the b_1^0, h_1 Reggeons, respectively. Regge cut amplitudes are incorporated into some models and are interpreted as rescattering of on-shell meson-nucleon amplitudes. The phases between the different poles and cuts can be critical in determining the polarizations and the constructive or destructive interferences that can appear. Four models are considered here.

The oldest model developed by Goldstein and Owens [5] has the exchange of leading Regge trajectories with appropriate t-channel quantum numbers along with Regge cuts generated via final state rescattering through Pomeron exchange. The Regge couplings to the nucleon were fixed by reference to electromagnetic form factors, $SU(3)_{flavor}$, and low energy nucleon-nucleon meson exchange potentials. At the time, the range of applicability was taken to be s above the resonance region and $\mid t \mid \leq 1.2\,\mathrm{GeV}^2$. Here we will let the $\mid t \mid$ range extend to large $\mid t \mid$ in order to see the predicted cross section dips from the zeroes in Regge residues. While the dip near $t \approx -0.5$ GeV^2 is present in π^0 data, it is not in the recent beam asymmetry data on η photoproduction [6]. This is not explained by the standard form of the "wrong signature" Regge residues.

Subsequently, somewhat similar approaches were developed. Quite recently, Mathieu *et al.* [7] (JPAC) (see also [8]), used the same set of Regge poles, but a simplified form of only ω -Pomeron cuts. They show that daughter trajectories are not significant as an alternative to the Regge cuts. However, to explain the lack of $t \approx -0.5$ GeV^2 dip in η photoproduction, they remove the standard wrong signature zero, *ad hoc*. Donnachie and Kalashnikova [9] have included t-channel ρ^0, ω, and the b_1^0, but not the h_1 Reggeon, all with different parameterizations from Ref. [5]. They include $\omega, \rho \times$ Pomeron cuts, as well as $\omega, \rho \times f_2$ lower lying cuts, which help to fill in the wrong signature zeroes of the ω, ρ Regge pole residues. The model of Laget and collaborators [10] included u-channel baryon exchange. That model also connected the small and large t-channel regimes by a mechanism called "saturating" the Regge trajectories at

* Now at the Institut für Kernphysik, Forschungszentrum Jülich, 52424 Jülich, Germany
† Corresponding author; mamaryan@odu.edu

$\alpha(t) \rightarrow -1$ for $t < -1.5$ GeV^2, thereby describing the full angular range ($\theta = 0 - 2\pi$), while the other models are good for different ranges of the forward direction, i.e., from $|t| = -t_{min}$ at $\theta = 0$ to $\theta = \pi/2$, where t is the squared four-momentum transfer [5, 7, 9]. Here, we examine how Regge phenomenology works for the energy range of 2.8 GeV $<$ E$_\gamma$ $<$ 5.5 GeV.

The introduction of the handbag mechanism, developed by Kroll *et al.* [11], has provided complimentary possibilities for the interpretation of hard exclusive reactions. In this approach, the reaction is factorized into two parts, one quark from the incoming and one from the outgoing nucleon participate in the hard sub-process, which is calculable using pQCD. The soft part consists of all the other partons that are spectators and can be described in terms of GPDs [12]. This approach was developed to understand the nature of the observation which the HERMES Collaboration made [13]. The handbag model applicability requires a hard scale, which, for meson photoproduction, is only provided by large transverse momentum. That corresponds to large angle production, roughly for $-0.6 \leq \cos\theta \leq 0.6$. Here, we examined how the handbag model may extend for the $\gamma p \rightarrow p\pi^0$ case as Kroll *et al.* proposed. The distribution amplitude for the quark+antiquark to π^0 is fixed by other phenomenology and contributes to orders of magnitude short-fall.

Binary reactions in QCD, with large momentum transfer occur via gluon and quark exchanges between colliding particles. The constituent counting rules of Brodsky and Farrar [3] has a simple recipe to predict the energy dependence of the differential cross sections of two-body reactions at large angles when t/s is finite and is kept constant. The lightest meson photoproduction was examined in terms of the counting rules [14–18]. As has been observed, first of all at SLAC by Anderson *et al.*, the reaction $\gamma p \rightarrow \pi^+ n$ shows agreement with constituent counting rules that predict the cross section should vary as s^{-7} [14]. The agreement extends down to s = 6 GeV^2 where baryon resonances are still playing a role. Here, we examined how the counting rule is applicable to the $\gamma p \rightarrow \pi^0 p$ up to s = 10 GeV^2.

Previous bremsstrahlung measurements, for $2 \leq E \leq 18$ GeV (1964 – 1979) gave 451 data points $d\sigma/dt(|t|)$s for $\gamma p \rightarrow p\pi^0$ [19], have very large systematic uncertainties and do not have sufficient accuracy to perform comprehensive phenomenological analyses. A previous CLAS measurement has an overall systematic uncertainty of 5% and its contribution for $2.0 \leq E \leq 2.9$ GeV is limited to 164 $d\sigma/dt(|t|)$s [20].

The new measurement, presented here, currently is the only measurement that bridges resonance and high energy, both narrow and wide angles, regions of exclusive π^0 photoproduction. This significantly extends the available database, facilitating the examination of the resonance, "Regge", and wide angle QCD regimes of phenomenology. The broad range of c.m. energy, $\sqrt{s}$, is particularly helpful in sorting out the phenomenology associated with both Regge and QCD-based models of the nucleon [4].

In this work, we provide a large set of differential cross section values from $E = 1.275 - 5.425$ MeV in laboratory photon energy, corresponding to a range of c.m. energies, $W = 1.81 - 3.33$ GeV. We have compared the Regge pole, the handbag, and the constituent counting rule phenomenology with the new CLAS experimental information on $d\sigma/dt(|t|)$ for the $\gamma p \rightarrow \pi^0 p$ reaction above the "resonance" regime. As will be seen, this data set quadruples the world bremsstrahlung database above E = 2 GeV and constrains the high energy phenomenology well with previous a CLAS measurement [20].

The experiment was performed during March-June, 2008 with the CLAS setup at TJNAF using a tagged photon beam produced by bremsstrahlung from the 5.72 GeV electron beam provided by the CEBAF accelerator, which impinged upon a liquid hydrogen target. The experiment as a whole was a set of different experiments running at the same time with the same experimental conguration (cryogenic target, tagger, trigger conguration, and CLAS) and was designated with the name "g12". Particle identication for the experiment was based on vs. momentum×charge. The experimental details are given in Ref. [21]. The reaction of interest is the photoproduction of neutral pions on a hydrogen target $\gamma p \rightarrow p\pi^0$, where the neutral pions were detected via external conversion, $\pi^0 \rightarrow \gamma\gamma \rightarrow e^+e^-\gamma$ and subsequent Dalitz decay $\pi^0 \rightarrow \gamma^*\gamma \rightarrow e^+e^-\gamma$. Running the experiment at high beam current was possible due to the final state containing three charged tracks, $p; e^+; e^-$, as opposed to single prong charged track detection, which impose limitations due to trigger and data acquisition restrictions.

Lepton identification was based on conservation of the π^0 mass. Once the data was skimmed for p, π^+, π^-, all particles that were π^+, π^- were tentatively assigned to be electrons or positrons based on their charge (for details, see Ref. [22]). After particle selection, standard $g12$ calibration, fiducial cuts [21] and timing cuts were applied in the analysis.

The analysis employed three separate kinematic fitting hypotheses, 4-C, 1-C, and 2-C, as well as a cut on the missing energy of the detected system. The 4-C fit used the $\gamma p \rightarrow p\pi^+\pi^-$ channel to filter background from double charged pion production from single π^0 production. The 1-C fit was used for the topology of $\gamma p \rightarrow pe^+e^-(\gamma)$ to fit to a missing final state photon. The 2-C fit was used for the topology of $\gamma p \rightarrow pe^+e^-(\gamma)$ to fit to a missing final state photon but also to constrain the invariant mass of $e^+e^-(\gamma)$=m$^2_{\pi^0}$. The values of the "condence levels" cuts employed was determined using statistical signicance to get the best signal/background ratio. The "confidence levels" for each constraint were consistent between $g12$ data and Monte-Carlo simulations. Monte-Carlo generation was performed using the PLUTO++ package developed for the HADES Collaboration [23].

The remainder of the background was attributed to $\pi^+\pi^-$ events. To reduce the background further, a comparison of the missing mass squared off the proton and

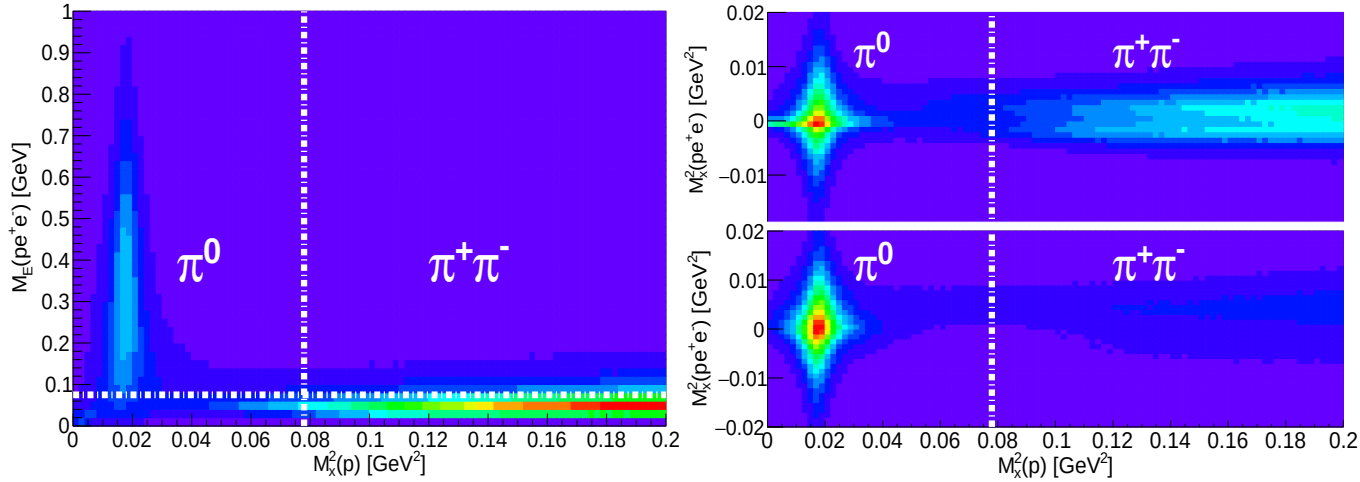

FIG. 1: (Color online)(left panel)M_x^2(p) vs. $M_E(pe^+e^-)$. (Right panel)M_x^2(p) vs. $M_x^2(pe^+e^-)$;(right-top panel) before applying the $M_E(pe^+e^-) < 75$ MeV condition, (right-bottom panel) after applying the $M_E(pe^+e^-) < 75$ MeV condition. The horizontal white dashed-dotted line depicted on the left panel illustrates the 75 MeV threshold used in this analysis. The vertical white dashed-dotted line depicts the kinematic threshold for $\pi^+\pi^-$ production.

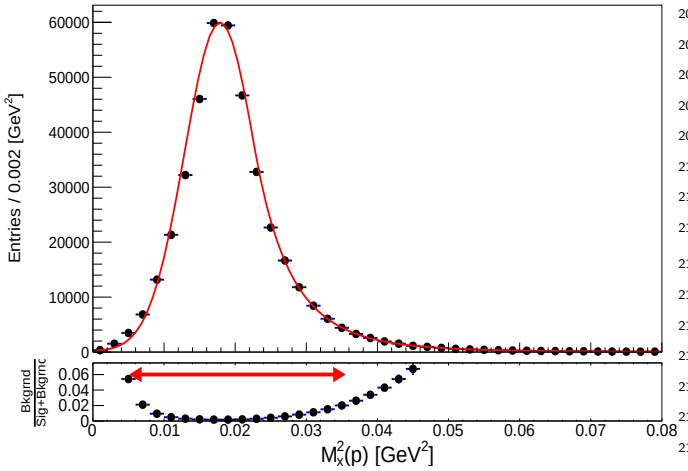

FIG. 2: (Color online) (top-panel) Peak of π^0 in the missing mass of proton for events with $pe^+e^-(\gamma)$ in the final state. The red-solid line depicts the fit function (signal+background). (bottom-panel) Relative contributions of $\frac{\text{Background}}{\text{Signal+Background}}$. The red arrow indicates the cut placed on the $M_x^2(p)$ distribution to select π^0 events.

the pe^+e^- missing energy of the system was performed, see Fig. 1. This comparison revealed that the majority of $\pi^+\pi^-$ background has missing energy less than 75 MeV. To eliminate this background all events with a missing energy less than 75 MeV were removed.

The distribution of the proton missing mass for events with $pe^+e^-(\gamma)$ in the final state is shown in Fig. 2. A fit is performed with the Crystal Ball function [24, 25] for the signal, plus a 3rd order polynomial function for the background. The total signal+background is shown by a red solid line. The fit results in $M_{\pi^0}^2 = 0.0179$ GeV^2 and the Gaussian σ=0.0049 GeV^2. To select π^0 events, an asymmetric cut, from the measured mean value, was placed in the range $0.0056 \leq M_x^2(p) \leq 0.035$. This cut range can be seen as the red arrow in the bottom panel of Fig. 2 along with the ratio of background events to the total number of events. As shown in Fig. 2, the event selection strategy for this analysis allowed to have a negligible integrated background of no more than $\sim 1.05\%$.

Overall the systematic uncertainty is independent of the production angle and varies between 9% and 12% as a function of energy. The individual contributions came from particle efficiency, sector-to-sector efficiency, flux determination, missing energy cut, 4-C, 2-C, and 1-C probabilities, target length, branching ratio, fiducial cut, and the z-vertex cut. The largest contributions to the systematic uncertainties were the sector-to-sector (4.4 – 7.1%), flux determination (5.7%), and the cut on the 1-C t pull probability (1.6 – 6.1%). All systematic uncertainties and there determinations are described in Ref. [22].

The new CLAS high statistics cross sections, presented here, for $\gamma p \rightarrow \pi^0 p$ are compared in Figs. 3 and 4 with data from previous CLAS measurements [20], and bremsstrahlung DESY, Cambridge Electron Accelerator (CEA), and SLAC, and Electron Synchrotron at Cornell Univ. experiments [19]. The overall agreement is good, particularly with the previous CLAS data.

At higher energies (above $s \sim 6$ GeV^2) and large c.m. angles ($\theta \geq 90^\circ$) in c.m., the results are consistent with the s^{-7} scaling, at fixed t/s, as expected from the constituent counting rule [3]. The black dash-dotted line at 90° (Fig. 3) is a result of the fit of new CLAS $g12$ data only, performed with a power function $\sim s^{-n}$, leading to n = 6.89±0.26. Oscillations observed at 50° and 70° up to s∼10 GeV^2 indicate that the constituent counting rule requires higher energies and higher $|t|$ before it can provide a valid description.

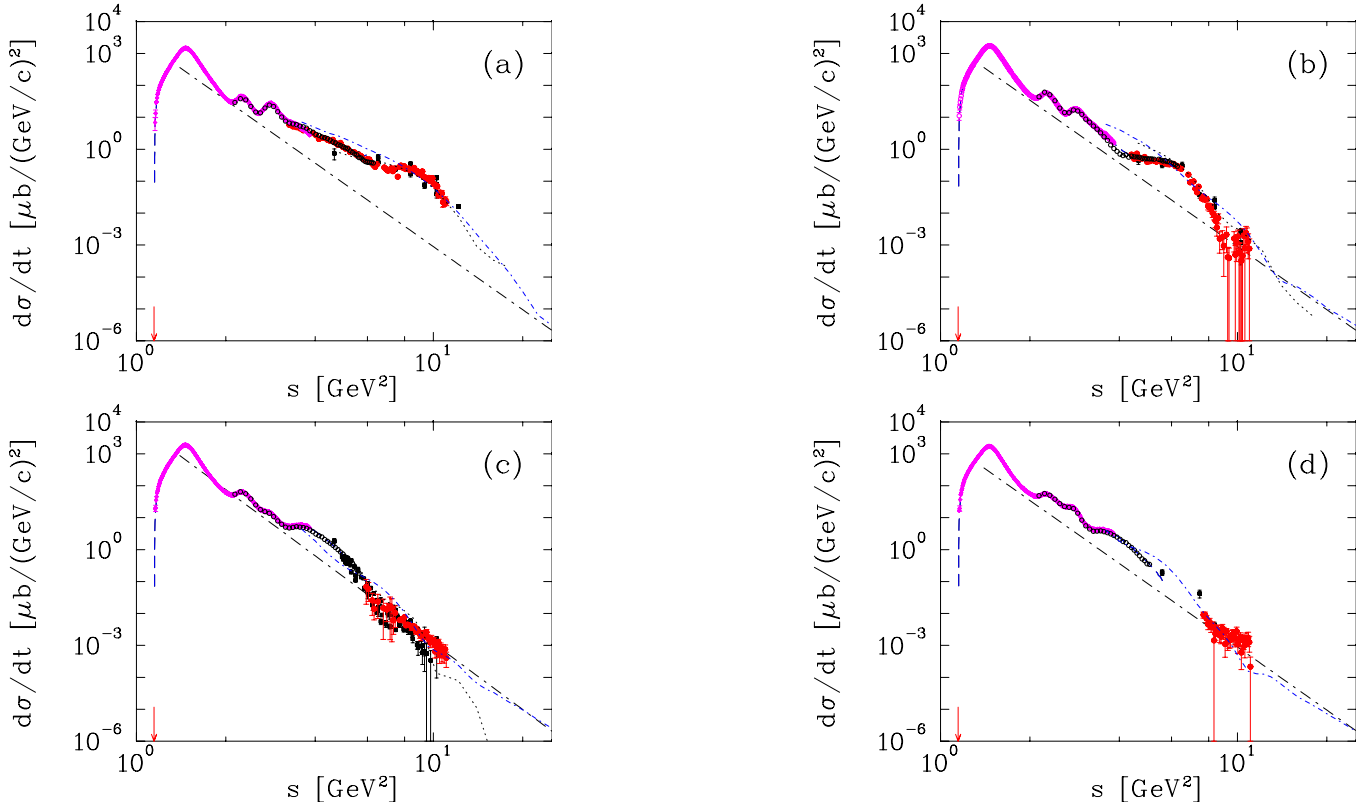

FIG. 3: (Color online) Differential cross section of $\gamma p \to \pi^0 p$ $d\sigma/dt(s)$ at polar angles of (a) 50°, (b) 70°, (c) 90°, and (d) 110° in the c.m. frame as a function of c.m. energy squared, s. The red filled circles are the current $g12$ CLAS data. The recent tagged data are from previous CLAS Collaboration measurements [20] (black open circles) and the A2 Collaboration at MAMI [26] (magenta open diamonds with crosses). While black open filled squares are data from old bremsstrahlung measurements above E = 2 GeV [19]. Plotted uncertainties are statistical. The blue dashed line corresponds to the SAID PWA PR15 solution (no new CLAS $g12$ data are used for the fit) [26]. Black dot-dashed lines are plotted as the best fit result for the spectrum at 90°. Pion production threshold shown as a vertical red arrow. Regge results [5, 10] are given by black dotted and blue dash-dotted, respectively.

In Figs. 4 and 5, the $d\sigma/dt(|t|)$ values are shown along with predictions from Regge pole and cut [5, 7, 9, 10] models and the handbag [11] model.

Below $|t| \sim 0.6$ GeV^2 there is a small difference between different Regge approaches. Overall, the Regge approximation becomes less relevant below E = 3 GeV (Fig. 4). This CLAS data make this statement more apparent. Note that some small structures start to appear around $|t| = 0.3 - 0.6$ GeV^2 ($\cos\theta = 0.6 - 0.8$) below E = 4 GeV. This is surprising since there was no previous indication of this dip, in data, prior to this measurement. Note that the Regge amplitudes imposes non negligible constraints for the "resonance" region. Our data show two more visible dips above E = 4 GeV and around $|t| \sim 3$ GeV^2 and $|t| \sim 5$ GeV^2, where the Regge models [5, 9, 10] predict incorrect signature zeroes, this is where the Regge trajectories cross negative even integers. For the dominant vector meson Regge poles, these dips should appear at approximately $-t = 0.6$, 3.0, 5.0 GeV^2, which agrees with the data. The description of the π^0 photoproduction cross sections at largest $|t|$ requires some improvement of the Regge model probably by including u-channel exchange.

Fig. 5 shows that the new CLAS data are orders of magnitude higher than the handbag model for π^0 photoproduction below $s = 11$ GeV^2 (blue double solid line).

Through the experiments described above, an extensive and precise data set (2030 data points) on the differential cross section for π^0 photoproduction from the proton has been obtained over the range of $1.81 \leq W \leq 3.33$ GeV. A novel approach based on the use of the Dalitz decay mode was employed for extracting the cross sections from the experimental data. Measurements are performed in the reaction $\gamma p \to p e^+ e^- X(\gamma)$ using a tagged photon beam spanning the energy interval covered by "resonance" and "Regge" regimes.

The measurements obtained here have been compared to existing data. The overall agreement is good, while the data provided here quadrupled the world bremsstrahlung database above E = 2 GeV and covered the previous reported energies with finer resolution. By comparing this new and greatly expanded data set to the predictions of several phenomenological models, the present data were found to support the Regge pole model and

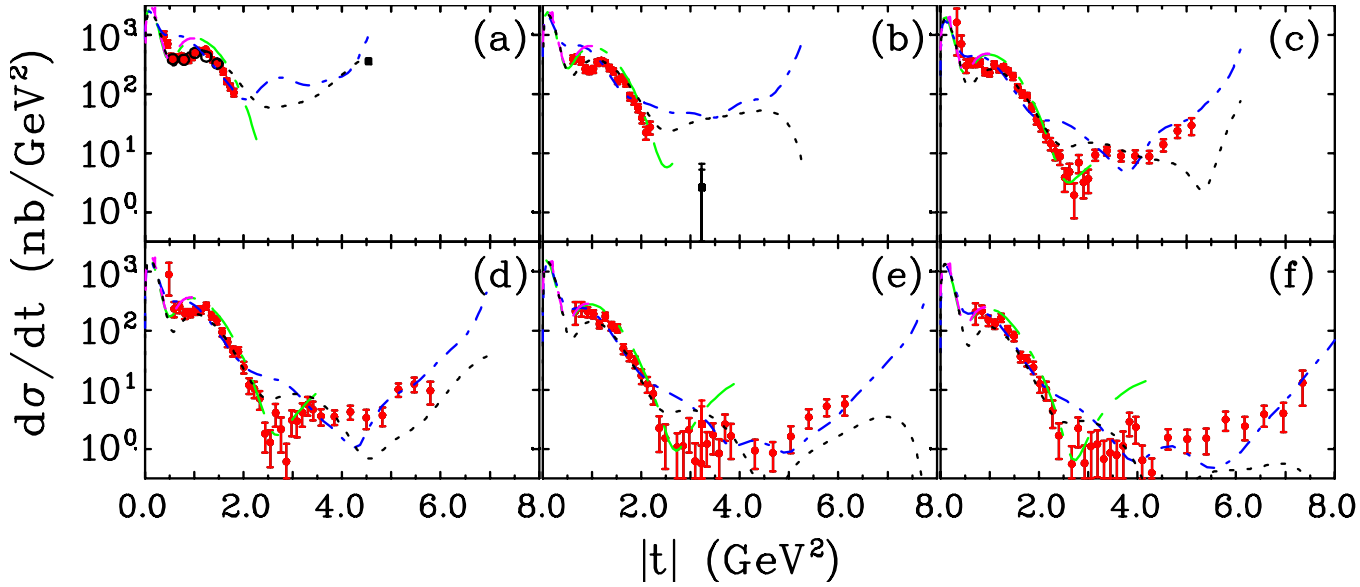

FIG. 4: (Color online) Samples of the π^0 photoproduction cross section, $d\sigma/dt(|t|)$, off the proton versus $|t|$ above "resonance" regime. (a) E = 2825 MeV and W = 2490 MeV, (b) E = 3225 MeV and W = 2635 MeV, (c) E = 3675 MeV and W = 2790 MeV, (d) E = 4125 MeV and W = 2940 MeV, (e) E = 4575 MeV and W = 3080 MeV, and (f) E = 4875 MeV and W = 3170 MeV. Tagged experimental data are from the current CLAS $g12$ (red filled circles) and a previous CLAS measurement [20] (black open circles). The plotted points from previously published bremsstrahlung experimental data above E = 2 GeV [19] (black filled squares) are those data points within $\Delta E = \pm 3$ MeV of the photon energy in the laboratory system indicated on each panel. The uncertainties plotted are only statistical. Regge results [5, 7, 9, 10] are given by black dotted, blue short dash-dotted, green long dash-dotted, and magenta long dashed lines, respectively.

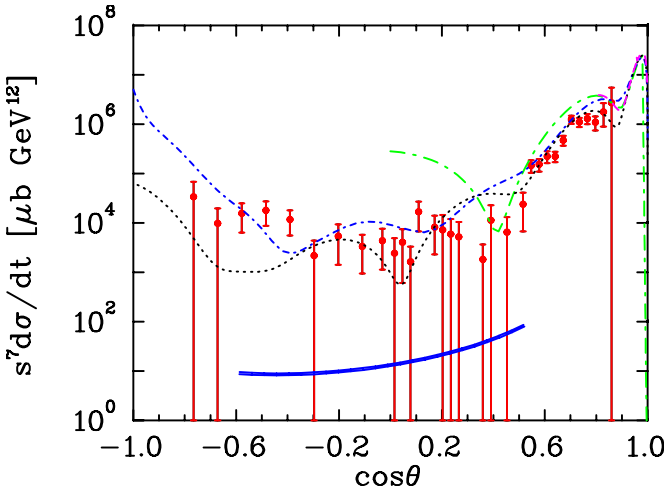

FIG. 5: (Color online) Differential cross section of π^0 photoproduction. The CLAS experimental data at $s = 11$ GeV^2 are from the current experiment (red filled circles). The theoretical curves for the Regge fits are the same as in Fig. 4 and the handbag model by Kroll *et al.* [11] (blue double solid line).

the constituent counting rule while disfavoring the handbag approach.

The results presented in this paper form part of the PhD dissertation of Michael C. Kunkel. We thank Stanley Brodsky, Alexander Donnachie, Peter Kroll, Jean-Marc Laget, Vincent Mathieu, and Anatoly Radyushkin for discussions of our measurements. We would like to acknowledge the outstanding efforts of the staff of the Accelerator and the Physics Divisions at Jefferson Lab that made the experiment possible. This work was supported in part by the Italian Istituto Nazionale di Fisica Nucleare, the French Centre National de la Recherche Scientifique and Commissariat à l'Energie Atomique, the United Kingdom's Science and Technology Facilities Council (STFC), the U. S. DOE and NSF, and the Korea Science and Engineering Foundation. The Southeastern Universities Research Association (SURA) operates the Thomas Jefferson National Accelerator Facility for the US DOE under contract DEAC05–84ER40150.

[1] J. P. Ader, M. Capdeville, and P. Salin, Nucl. Phys. B **3**, 407 (1967).

[2] H. K. Armenian, G. R. Goldstein, J. P. Rutherfoord, and D. L. Weaver, Phys. Rev. D **12**, 1278 (1975).

[3] S. J. Brodsky and G. R. Farrar, Phys. Rev. Lett. **31**, 1153 (1973).

[4] P. Kroll, Eur. Phys. J. A **53**, no. 6, 130 (2017) and references therein.

[5] G. R. Goldstein and J. F. Owens, Phys. Rev. D **7**, 865 (1973).

[6] H. Al Ghoul *et al.* [GlueX Collaboration], Phys. Rev. C **95**, no. 4, 042201 (2017).

[7] V. Mathieu, G. Fox, and A. P. Szczepaniak, Phys. Rev. D **92**, no. 7, 074013 (2015); J. Nys *et al.* [JPAC Collaboration], Phys. Rev. D **95**, no. 3, 034014 (2017).

[8] V. L. Kashevarov, M. Ostrick, and L. Tiator, arXiv:1706.07376 [hep-ph].

[9] A. Donnachie and Y. S. Kalashnikova, Phys. Rev. C **93**, no. 2, 025203 (2016).

[10] J. M. Laget, Phys. Rev. C **72**, 022202 (2005); M. Guidal, J. M. Laget, and M. Vanderhaeghen, Nucl. Phys. A **627**, 645 (1997).

[11] H. W. Huang and P. Kroll, Eur. Phys. J. C **17**, 423 (2000); H. W. Huang, R. Jakob, P. Kroll, and K. Passek-Kumericki, Eur. Phys. J. C **33**, 91 (2004); M. Diehl and P. Kroll, Eur. Phys. J. C **73**, no. 4, 2397 (2013).

[12] X. D. Ji, Phys. Rev. D **55**, 7114 (1997); A. V. Radyushkin, Phys. Lett. B **380**, 417 (1996); A. V. Radyushkin, Phys. Rev. D **56**, 5524 (1997); D. Müller, D. Robaschik, B. Geyer, F.-M. Dittes, and J. Horejsi, Fortsch. Phys. **42**, 101 (1994).

[13] M. Amarian *et al.* [HERMES Collaboration], DESY-HERMES-00-47; AIP Conf. Proc. **570**, 428 (2001), Proceedings of the *14th International Spin Physics Symposium* (SPIN 2000), Osaka, Japan, Oct. 2000, edited by K. Hatanaka, T. Nakano, K. Imai, and H. Ejiri.

[14] R. L. Anderson, D. Gustavson, D. Ritson, G. A. Weitsch, H. J. Halpern, R. Prepost, D. H. Tompkins, and D. E. Wiser, Phys. Rev. D **14**, 679 (1976).

[15] D. A. Jenkins and I. I. Strakovsky, Phys. Rev. C **52**, 3499 (1995).

[16] L. Y. Zhu *et al.* [Jefferson Lab Hall A Collaboration], Phys. Rev. Lett. **91**, 022003 (2003).

[17] W. Chen *et al.*, Phys. Rev. Lett. **103**, 012301 (2009).

[18] K. J. Kong, T. K. Choi, and B. G. Yu, Phys. Rev. C **94**, no. 2, 025202 (2016).

[19] The Durham HEP Reaction Data Databases (UK) (Durham HepData): http://durpdg.dur.ac.uk/hepdata/reac.html .

[20] M. Dugger *et al.*, Phys. Rev. C **76**, 025211 (2007).

[21] G12 experimental group, CLAS-NOTE 2017 - 002, 2017 `https://misportal.jlab.org/ul/Physics/Hall-B/clas/viewFile.cfm/2017-002.pdf?documentId=756`.

[22] M. C. Kunkel, CLAS-NOTE 2017 - 005, 2017 `https://misportal.jlab.org/ul/Physics/Hall-B/clas/viewFile.cfm/2017-005.pdf?documentId=767`.

[23] I. Frohlich *et al.*, PoS ACAT , 076 (2007) [arXiv:0708.2382 [nucl-ex]].

[24] M. Oreglia, SLAC Stanford - SLAC-236 (80,REC.APR. 81) 226p; Ph. D. Thesis, SLAC, 1980.

[25] T. Skwarnicki, DESY-F31-86-02, DESY-F-31-86-02; Ph. D. Thesis, Inst. Nucl. Phys. Cracow, Poland, 1986.

[26] P. Adlarson *et al.* [A2 Collaboration at MAMI], Phys. Rev. C **92**, no. 2, 024617 (2015).